A vortex method for viscous unsteady flows

P. K. Dutta

Computational and Theoretical Fluid Dynamics Division
National Aerospace Laboratories, Bangalore 560 017, INDIA

Abstract: A simple method is presented for the creation of vorticity from a solid boundary in the form of discrete vortex blobs. These vortices have uniform-vorticity cores and are released from a number of points distributed around the body surface at a small distance away from the surface. Their strengths are obtained by satisfying the no-slip condition at the midpoints of the corresponding vortex sheets. The dynamics of these vortices is then considered by including the effect of viscous diffusion by random walk approach. The method is applied to the starting flow past a circular cylinder. A detailed parametric study shows that viscosity has the most significant effect on the computed results and, in order to obtain meaningful results, it must be reduced suitably to compensate for the artificial viscosity arising from numerical integration of equations of motion of the discrete vortices. Results are obtained for three typical Reynolds numbers of 9500, 3000 and 550, and are found to be in very good agreement with experimental measurements for the centerline velocity distribution. In particular, the case of Re=550 illustrates the usefulness of the present model even at low Reynolds numbers. The vortex patterns, velocity vectors and particle path lines also conform to the experimental flow visualization pictures. Though the method is developed for a simple configuration like a circular cylinder, it can be easily extended to any general body shape.

1. Introduction

Viscous incompressible flow past a solid body is governed by the Navier-Stokes equations subject to the conditions of no slip and zero normal velocity on the body surface. Dynamics of such flows is better understood when one considers the equivalent vorticity equations in a Lagrangian frame of reference. For two-dimensional flows, these equations imply that the vorticity associated with a fluid particle changes due to viscous diffusion alone, while the no-slip condition provides a mechanism for creation of vorticity from a solid surface. A convenient method that uses the above idea to simulate the temporal evolution of two-dimensional viscous unsteady flows is provided by the discrete vortex model. The essential steps in this method consist of (a) creation of discrete vortex sheets or blobs from the body surface by satisfying the no-slip condition, (b) convection of discrete vortices with their local velocities and finally (c) viscous diffusion of vortices by random walk method (Chorin 1973). The method was first applied by Rosenhead (1931) to the problem of vortex sheet roll-up and has now reached a stage where it is being applied to complex flows involving large scale separation and turbulence (Dutta 1988). The method has certain distinct advantages over the finite-difference or finite-element methods used to solve the Navier-Stokes equations. Firstly, the method can be easily applied to a complex body geometry (*e.g.*, multi-element airfoils) since it is a grid free method. Secondly, the method simulates convection very accurately since the fluid particles having vorticity are moved with their local velocities. Thirdly, the far field boundary condition is satisfied exactly. Finally, the method provides an economical description of the flow field at high Reynolds numbers when the vorticity is restricted to narrow regions like boundary layers, wakes, mixing

layers and jets and, hence, can be resolved more accurately. However, the method requires a large number of discrete vortices to simulate viscous effect (Milinazo and Saffman 1977) and, hence, requires large computation time which is proportional to the square of the number of vortices. The usefulness and limitations of the method are discussed in detail in a number of reviews (Clements and Maull 1975, Clements 1977, Saffman and Baker 1979, Maull 1979, Leonard 1980, Sarpkaya 1989).

A major source of difficulty in discrete vortex method has been the choice of certain parameters which are required for numerical simulation of a given flow field. In reality, vorticity Is created from a body surface in the form of a vortex sheet wrapped around the body, so as to nullify any nonzero slip velocity. For numerical computation, this sheet is discretized into a number of discrete vortex blobs whose strength and location are such that the no-slip condition is satisfied at the corresponding control points on the body surface. In practice, the location of these vortices is prescribed so that their strength can be obtained by satisfying the above condition. Since the computed results often depend on the choice of location of vortex release points, it is necessary that these locations are chosen appropriately to reflect the true state of the flow near the body surface. It is to this aspect that the present work addresses itself by considering the starting flow past a circular cylinder.

The impulsively started flow past a circular cylinder has received considerable attention due to its simple geometry and a variety of complex flow regimes observed experimentally with increasing times and Reynolds numbers (Honji and Taneda 1969, Taneda 1977, Tritton 1977, Coutanceau and Bouard 1977a,b, Bouard and Coutanceau 1980, Nagata *et al.* 1989,1990, Chu and Liao 1992). The most interesting features of the flow here are the primary and secondary vortices formed at Reynolds numbers above about 60 and a third vortex above a Reynolds number of about 5000. The accuracy of any computation can therefore be judged against the prediction of such features. Application of discrete vortex method to this problem was first reported by Chorin (1973) for Reynolds numbers ranging from 100 to 10000 and then by Cheer (1983) who used discrete vortex sheets near the body surface in order to resolve the flow field accurately. Smith and Stansby (1988) used the vortex-in-cell technique to obtain the velocity field with less computation time. A variant of this method was developed by Stansby and Smith (1989) who removed from computation the vortices which hit the cylinder. Kamemoto and Kawamata (1986) carried out boundary layer calculations upto the separation point from which vortices were released with properties based on the boundary layer characteristics. Recently, Ling *et al.*. (1992) used a hybrid method where the near field was obtained by solving the Navier-Stokes equations and only the far field away from the body surface was treated by discrete vortex method.

2. Computational method

Consider a circular cylinder of radius R placed in a stationary fluid having kinematic viscosity ν, such that the centre of the cylinder lies at the origin of the complex plane $z = x + iy$ (Fig. 1). At time $t = 0$, the fluid is suddenly set to motion along the x axis with a constant velocity U_∞. The Reynolds number for this flow is defined by $Re = U_\infty D/\nu$, where $D = 2R$ *is* the diameter of the cylinder. As already noted, the temporal evolution of this flow from time $t = 0$ is simulated by repeating the three basic processes - (a) releasing discrete vortex blobs from prescribed points on the cylinder surface by satisfying the no-slip condition, (b) convecting these vortices with their local velocities, and (c) adding viscous correction according to the random walk method (Chorin 1973). Suppose that at time $t > 0$, the flow field consists of N discrete vortices at Zj with circulation Tj and uniform-vorticity circular core of radius $'Rj$ where j varies from 1 to N. Following the

Biot-Savart law, the complex velocity $W(z)$ at any field point z can then be written as

$$W(z) = u - iv = U_\infty \left(1 - \frac{R^2}{z^2}\right) - \sum_{j=1}^{N} \frac{i\Gamma_j}{2\pi} \left[\frac{\bar{z} - \bar{z}_j}{\max\left(|z - z_j|^2, R_j^2\right)} - \frac{1}{z - R^2/\bar{z}_j}\right] \quad (1)$$

where the overbar implies complex conjugate. The equations of motion of the vortices, in the absence of viscous effect, are then given as

$$\frac{dz_k}{dt} = W(z_k) \quad (2)$$

where k also varies from 1 to N. These equations can be solved for given initial conditions at time t so as to obtain the vortex patterns in terms of z_k after a small time step δt. Using the simplest integration scheme, namely the first-order Euler scheme, one can then write, for the fc-th vortex,

$$\bar{z}_k(t + \delta t) = \bar{z}_k(t) + W(z_k)\,\delta t \quad (3)$$

where W at time t is given by Eq. (1). Following the random walk method of Chorin (1973), the effect of viscous diffusion is simulated by displacing the vortices by small amounts in both x and y directions. The Eqs. (3) are thus modified as

$$\bar{z}_k(t + \delta t) = \bar{z}_k(t) + W(z_k)\,\delta t + (\tilde{x}_k - i\tilde{y}_k) \quad (4)$$

where x_k and y_k are two independent sets of Gaussian random numbers corresponding to the k-th vortex and have mean 0 and standard deviation $\sqrt{2\nu\delta t}$. To avoid vortex cores crossing the cylinder surface at any time t, the vortices satisfying the condition $|z_k|^2 \leq (R + Rk)^2$ are removed from the flow field.

Knowing the vortex pattern at any time t, the instantaneous streamline starting from a point ZQ can be obtained by connecting the points $Z_0, Z_1, Z_2, \ldots$, where, for $j = 1, 2, \ldots$,

$$\bar{Z}_j = \bar{Z}_{j-1} + W(Z_{j-1})\,\delta t^* \quad (5)$$

Here, δt^* is a small time step selected in such a way that the streamline is as smooth as possible and the starting point ZQ is chosen so as to obtain the desired streamlines. Equation (1) can also be used to obtain the streamwise centerline velocity distribution u_c along the x axis in the wake. It may be noted that in irrotational flow, that exists before the first set of vortices is released into the flow, this velocity is given, from Eq. (1) with $N = 0$, as

$$u_c = U_\infty \left(1 - \frac{R^2}{x^2}\right) \quad (6)$$

The pressure coefficient Cp at a point z_b on the cylinder surface can also be obtained, from the unsteady Bernoulli equation (Batchelor 1970), as

$$C_P = \frac{p - p_\infty}{\frac{1}{2}\rho U_\infty^2} = \frac{1}{U_\infty^2}\left(U_\infty^2 - V_s^2 - 2\frac{\partial \phi}{\partial t}\right) \quad (7)$$

where p, V_s and ϕ are the pressure, tangential velocity and velocity potential at z_b, p_∞ is the freestream pressure and p is the fluid density. The tangential velocity V_s in clockwise direction around the body is here given by

$$V_s(z_b) = W(z_b)\frac{dz_b}{ds} = -iW(z_b)\exp(-i\theta) \quad (8)$$

where s = $R\theta$ is the arc length measured along the cylinder surface in clockwise dir ction and the angle 6 lying between 0 and 2π *is* defined such that (Fig. 1)

$$z_b(0) = R\exp(-i0) \tag{9}$$

When the discrete vortices do not intersect the cylinder surface, the time deriva ve of velocity potential ϕ is given, from Eq. (1), as

$$\frac{\partial w}{\partial t} = \frac{\partial \phi}{\partial t} + i\frac{\partial \psi}{\partial t} = \sum_{j=1}^{N} \frac{i\Gamma_j}{2\pi}\left[\frac{\dot{z}_j}{z - z_j} - \frac{\dot{\bar{z}}_j (R/\bar{z}_j)^2}{z - R^2/\bar{z}_j}\right] \tag{10}$$

where $w = \phi + i\psi$ is the complexpotential, ψ isthe stream function and z_j denots the velocity of the j-th discrete vortex. At time t = 0, before the first set of vortices is re eased into the flow, one thus obtains

$$C_P = 1 - 4\sin^2 0 \tag{11}$$

The lift and drag coefficients C_L and C_D are now given as

$$C_D + iC_L = -i \oint C_P \, d(z_b/D) \tag{12}$$

where the integration is carried out around the cylinder contour in clockwise directi n and the diameter D is chosen as the reference length. The integral in Eq. (12) can be eva uated analytically (Milne-Thomson 1968 and Graham 1980), after using Eqs. (7) and ( )), to give

$$C_D + iC_L = \frac{4\pi}{U_\infty^2 D}\sum_{j=1}^{N} \frac{i\Gamma_j}{2\pi}\left[\dot{\bar{z}}_j + \left(\frac{R}{\bar{z}_j}\right)^2 \dot{z}_j\right] \tag{13}$$

This expression shows that, for flows which are symmetric about the x axis, t e lift coefficient *CL* is identically zero. This provides a check for flow symmetry in nu erical computations.

The manner in which discrete vortices are created from the cylinder surface s now described. Let us suppose that, at time t, the tangential velocity V_s at a point z_b on the cylinder surface is nonzero (Fig. 2a). This velocity is nullified to satisfy the o-slip condition by wrapping a vortex sheet of strengtll $-V_s$ per unit length around the c linder (Fig. 2b). The vortex sheet is then discretized into N_{eb} vortex sheets of equal ength As = $\pi D/N_{eb}$ (Fig. 2c) such that the midpoint of the j-th discrete vortex sheet lie at

$$z_{bm,j} = z_b(\theta_{m,j}) \tag{14}$$

where

$$\theta_{m,j} = \frac{2\pi}{N_{eb}}\left(j - \frac{1}{2}\right) \tag{15}$$

The strength Γ_j^{**} of this vortex sheet is then given by

$$\Gamma_j^{**} = -\int_j V_s(z_b)\, ds \approx -V_s(z_{bm,j})\,\Delta s \tag{16}$$

where the integration is carried out over the j-th vortex sheet and N_{eb} is assume to be sufficiently large. This vortex sheet is now replaced by a circular vortex blob of s ength $\Gamma_j^* = \Gamma d\Gamma_j^{**}$ and uniform-vorticity core of radius $R_c^* = Rd(D/N_{eb})$with its cc tre at $z_j^* = z_{bm,j} + (D/N_{eb})\bar{\alpha}\exp(-i\theta_j)$. The nondimensional parameters 3, Γ and $\bar{R}$ de rmine the normal distance of the vortex from the corresponding midpoint, its strength a d core radius. It may be noted that, for $\bar{R}$ = 1, the vortex core just touches the cylinder rface,

while, for $\bar{R} < 1$, the vortex core lies well outside the surface. Moreover, for $\bar{R} < 1$ and $\bar{\Gamma} = 1$, the strength of the circular vortex equals that of the corresponding vortex sheet. In this case, each of the vortices and its image vortex are enough to nullify the slip velocity at the corresponding midpoint $z_{bm,j}$. The above process of vortex creation is carried out at time interval At which should be an integral multiple of time step δt used to integrate the equations of motion. The released vortices are then allowed to convect according to Eq. (4).

For a given Reynolds number Re, the computation for the present problem proceeds with the choice of physical parameters $\bar{d}$, $\bar{\Gamma}$, $\bar{R}$ and At and numerical parameters N_{eb} and δt. A detailed parametric study was carried out to find the effect of each of these parameters on the computed results and to arrive at suitable values for these parameters for the results presented in this paper. These are described "in the next section.

3. Results and discussion

The computation was carried out for three Reynolds numbers Re = 9500, 3000 and 550 for which detailed experimental results (Bouard and Coutanceau 1980) are available. The freestream velocity U_∞ and the cylinder diameter D were both chosen as unity so that all dimensional quantities could be assumed to have been nondimensionalized with respect to a length scale D and time scale D/U_∞. The Reynolds number Re, which turns out to be $1/\nu$, and all the parameters $\bar{d}$, $\bar{\Gamma}$, $\bar{R}$, At, N_{eb} and δt were varied independently to see their effect on the computed results. The result of this study can be summarized as follows.

1. The kinematic viscosity ν appears to have the most significant effect on the computed results. This is due to the artificial viscosity arising from the truncation error in numerical integration of equations of motion. Thus, kinematic viscosity has to be reduced appropriately to compensate for this error. In the present study, this reduction was found to be $O(\delta t^2)$.

2. The parameter $\bar{d}$ affects the vortex pattern considerably. However, the quantitative results do not change much when $\bar{d} \sim \sqrt{\nu \delta t}$.

3. Time interval At must be chosen sufficiently small; otherwise the wake is found to consist of very few vortices.

4. As long as the number of discrete vortices N_{eb} released at time interval At is chosen large, it does not have any effect on the final results. Care should be taken to see that the wake contains sufficient number of vortices.

5. Time step δt should be chosen very carefully. On the one hand, it should be chosen small so as to minimize numerical error. On the other hand, if it is chosen too small, the vortices lie close to the cylinder for a larger number of time steps δt and have more probability of hitting the cylinder surface and getting lost.

6. Both $\bar{\Gamma}$ and $\bar{R}$ can be chosen as unity. Small variation (about 20%) does not affect the results appreciably.

The above study was used to select all the parameters appropriately in order to obtain the final results. The values *of* some of these parameters which were used in the computation for all the three Reynolds number are as follows.

$$\text{At} = St = 0.01 \quad \text{and} \quad \bar{\Gamma} = \bar{R} = 1$$

For Re = 9500, N_{eb}, 3 and ν were chosen as 60, 0.049 and 0.00000526 respectively. The detailed results for this case are shown in Fig. 3. The vortex patterns at increasing times

t (Fig. 3a) show the formation of two compact vortices at times $t > 1$, beyond which secondary vortices are formed. The profiles of streamwise centreline velocity in the wake and pressure distribution on the cylinder surface at different times t are shown in Fig. 3(b). Good agreement with experimental results of Bouard and Coutanceau (1980) can be seen very clearly in this figure. Figures 3(c) and 3(d) show the comparison of computed vortex pattern, velocity vectors and particle traces with experimental flow visualization pictures at times $t = 1.6$ and 2.0. The close similarity between the two again proves the capability of the present model. The drag coefficient CD here increases from 0 at time $t = 0$ to about 1 at $t = 1.5$ and remains approximately constant thereafter.

Computed results for $Re = 3000$ are shown in Fig. 4. The parameters chosen for this case are $N_{eb} = 120$, $\bar{d} = 0.174$ and $v = 0.00023333$. As before, both qualitative and quantitative agreement with experimental results is excellent. The twin vortices in the wake here are bigger than the ones in the previous case due to stronger effect of viscous diffusion (Fig. 4a). Formation of secondary and even tertiary vortices is also clear from Figs. 4(c) and 4(d). The drag coefficient CD in this case increases from 0 to about 1.2 as t increases from 0 to 1.5 and then drops to 0.85 at time t — 2. Finally, results for a very low Reynolds number of 550 are shown in Fig. 5 after using $N_{eb} = 120$, $\bar{d} = 0.3$ and v — 0.00171818. The vortex patterns here (Fig. 5a) show the highly diffusive nature of the flow. The drag coefficient increases from 0 to 0.85 as time t increases from 0 to 2, It is interesting to note that, even at such a low Reynolds number, the present model leads to very good agreement with experimental results (Fig. 5b) for streamwise centreline velocity distribution. Since the discrete vortex method is known to be applicable for high Reynolds number flows, this agreement indicates the usefulness of the present model in simulating even low Reynolds number flows for which more accurate results are usually obtained by finite-difference method. A colour plot of vortex patterns at t=1.0, 1.5, and 1.9 is presented in Fig. 6 for $Re = 3000$ illustrating the formation of secondary and tertiary vortices at large times.

4. Conclusions

The main aim of the present discrete vortex model is to retain the simple methodology using circular vortex blobs and fix the required parameters appropriately in order to obtain meaningful results. It is found that most of the parameters can be chosen without any ambiguity. The only parameters that require careful selection are the effective kinematic viscosity, number of discrete vortices to be released at each time interval and the release point of these vortices. When these are selected suitably, the computed results are found to be in very good agreement with experimental results both qualitatively and quantitatively. Of particular interest is the agreement at low Reynolds number, which brings out the potential of the model for a wide range of Reynolds numbers. Though the method has been applied to the case of a circular cylinder, it can be easily extended to any general configuration.

References

Batchelor, G. K. (1970), *An introduction to fluid dynamics*, Camb. Univ. Press, London.

Bouard, R. and Coutanceau, M. (1980), "The early stage of development of the wake behind an impulsively started cylinder for $40 < Re < 10^4$," *J. Fluid Mech.*, bf 101, p.583.

Cheer, A. Y. (1983), "Numerical study of incompressible slightly viscous flow past blunt bodies and airfoils," *SIAMJ. Stat. Comp.*, 4, p.685.

Chorin, A. J. (1973), "Numerical study of slightly viscous flow," *J. Fluid Mech.*, 57, p.785.

Chu, C. -C. and Liao, Y. -Y. (1992), "A quantitative study of the flow around an impulsively started circular cylinder," *Expt. Fluids*, 13, p.146.

Clements, R. R. (1977), "Flow representation, including separated regions, using discrete vortices," *Comp. Fluid Dyn.*, AGARD LS-86, 5.1.

Clements, R. R. and Maull, D. J. (1975), "The representation of sheets of vorticity by discrete vortices," *Prog. Aero. Sci.*, 16, p.129.

Coutanceau, M. and Bouard, R. (1977a), "Experimental determination of the main features of the viscous flow in the wake of a circular cylinder in uniform translation. Part 1. Steady flow," *J. Fluid Mech*, 79, p.231.

Coutanceau, M. and Bouard, R. (1977b), "Experimental determination of the main features of the viscous flow in the wake of a circular cylinder in uniform translation. Part 2. Unsteady flow." *J. Fluid Mech.*, 79, p.257.

Dutta, P. K. (1988), "Discrete vortex method for separated and free shear flows," Ph.D. Thesis, Indian Institute of Science, Bangalore.

Graham, J. M. R. (1980), "The forces on sharp-edged cylinders in oscillatory flow at low Keulegan-Carpenter numbers," *J. Fluid Mech.*, 97, p.331.

Honji, H. and Taneda, S. (1969), "Unsteady flow past a circular cylinder," *J. Phys. Soc. Japan*, 27, p.1668.

Kamemoto, K. and Kawamata, Y. (1986), "Representation of two-dimensional boundary layers by discrete vortices," *Proc. Int. Conf. Comp. Mech.*, Tokyo, p.261.

Leonard, A. (1980), "Vortex method for flow simulation," *J. Comp. Phys.*, 37, p.289.

Ling, G. -C., Ling, G. -P. and Wang, Y. -P. (1992), "Domain decomposition hybrid method for numerical simulation of bluff body flows," *Science in China*, 35, p.977.

Maull, D. J. (1979), "An introduction to the discrete vortex method," IUTAM/IAHR Conf., Karlsruhe.

Milinazo, F. and Saffman, P. G. (1977), "The calculation of large Reynolds number two-dimensional flow using discrete vortices with random walk," *J. Comp. Phys.*, 23, p.380.

Milne-Thomson, L. M. (1968), *Theoretical hydrodynamics*, Macmillan & Co. Ltd, London.

Nagata, H., Nagase, I. and Ito, K. (1989), "Unsteady flows past a circular cylinder started impulsively in the Reynolds number range $500 < Re < 10^4$ (The structure of the vortex region and feeding mechanism of vorticity)," *JSME Int. J., Series II*, 32, p.540.

Nagata, H., Ito, K. and Taniguchi, T. (1990), "Unsteady flows past a circular cylinder started impulsively in the Reynolds number range $500 < Re < 10^4$ (The pressure distribution on the surface of the cylinder)," *JSME Int. J., Series II*, 33, p.501.

Rosenhead, L. (1931), "The formation of vortices from a surface of discontinuity," *Proc. Roy. Soc. A*, 134, p.170.

Saffman, P. G. and Baker, G. R. (1979), "Vortex interactions," *Ann. Rev. Fluid Mech.*, 11, p.95.

Sarpkaya, T. (1989), "Computational methods with vortices - The 1988 Freeman scholar lecture," *J. Fluid Engg.*, **111**, p.5.

Smith, P. A. and Stansby, P. K. (1988), "Impulsively started flow around a circular cylinder by the vortex method," *J. Fluid Mech.*, 194, p.45.

Stansby, P. K. and Smith, P. A. (1989), "Flow around a cylinder by the random vortex method," *Proc. 8th Int. Conf. Offshore Mech. Arctic Engg.*, The Hague, p.419.

Taneda, S. (1977), "Visual study of unsteady separated flows around bodies," *Prog. Aero. Sci.*, 17, p.287.

Tritton, D. J. (1977), *Physical fluid dynamics*, Van Nostrand Reinhold.

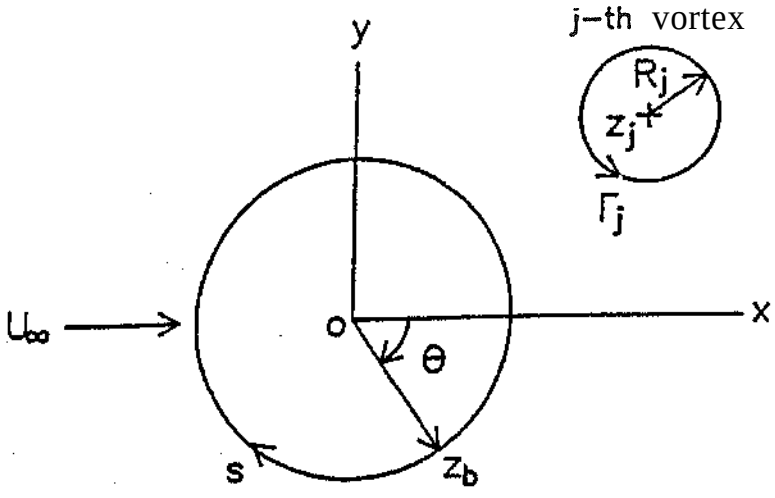

Fig. 1. Schematic diagram for uniform flow past a circular cylinder.

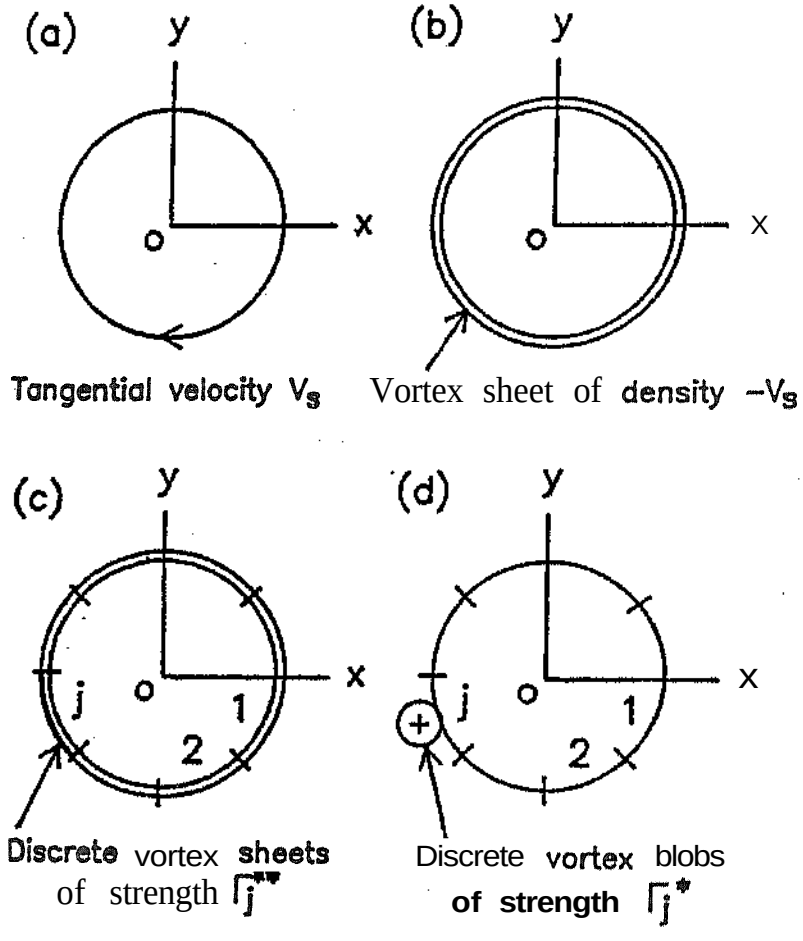

Fig. 2 Different stages of vortex creation from the body surface. (a) Before vortex creation, (b) cr ation vortex sheet, (c) creation of discrete vortex sheets and finally (d) creation of discrete vortex blobs.

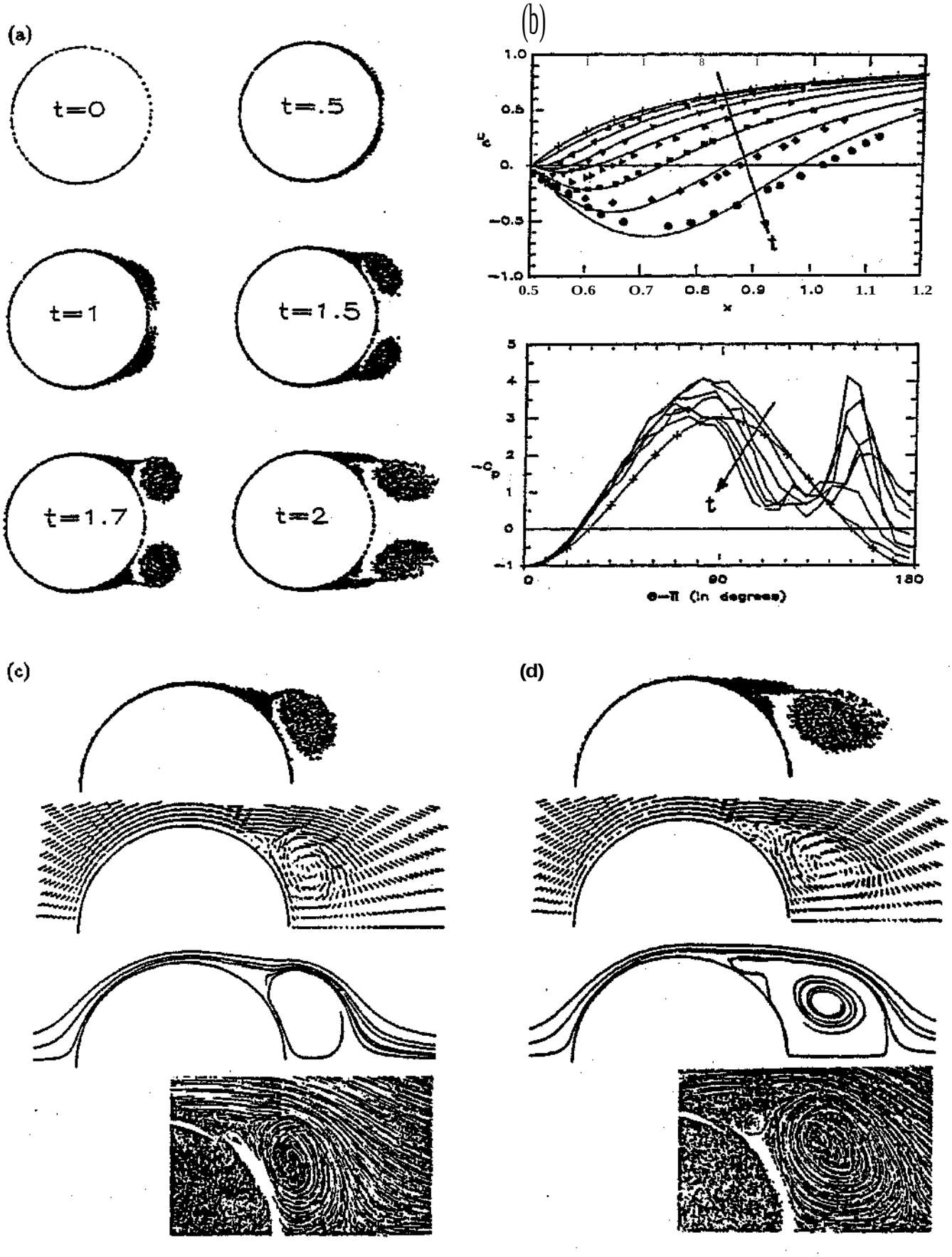

Fig. 3 Computed results for Ee = 9500. (a) Vortex patterns at times t, (b) distributions of streamwise centreline velocity u_e and pressure coefficient CP at times * = 0.5, 0.75, 1.0, 1.25, 1.5, 1.75 and 2.0 and comparison of vortex pattern, velocity vectors, particle traces and flow visualisation picture at times (c) $t = 1.6$ and (d) $t = 2.0$, Symbols indicate experimental data (Bouard and Coutanceau 1980) for u_e and potential flow distribution for C_P.

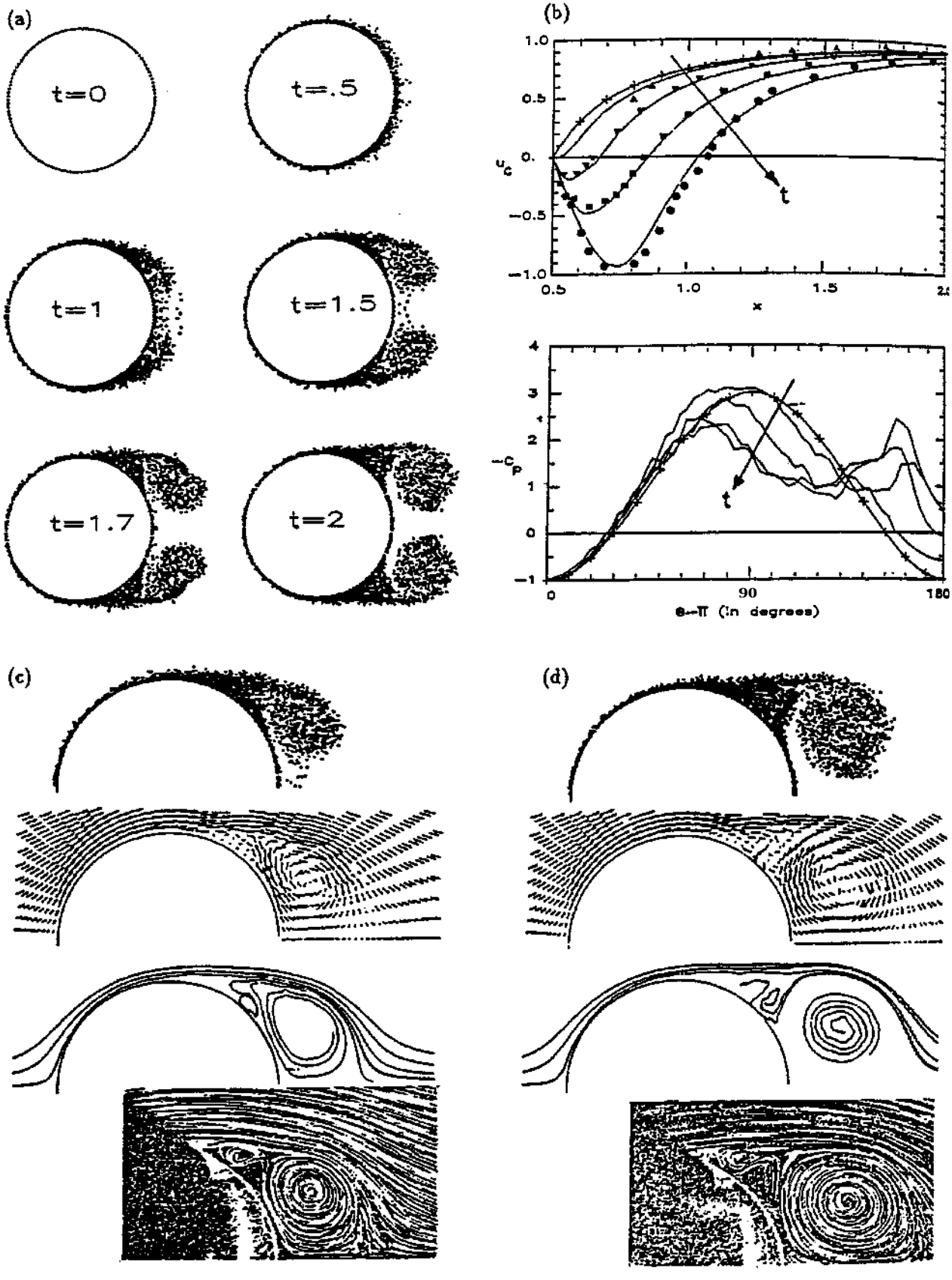

Fig. 4 Computed results for Re = 3000. (a) Vortex patterns at times t, (b) distributions of streamwise centreline velocity u_c and pressure coefficient *CP* at times t = 0.5, 1.0, 1.5, and 2.0 and comparison of vortex pattern, velocity vectors, particle traces and flow visualisation picture at times (c) t = 1.5 and (d) t = 2.0. Symbols indicate experimental data (Bouard and Coutanceau 1980) for u_c and potential flow distribution for C_P.

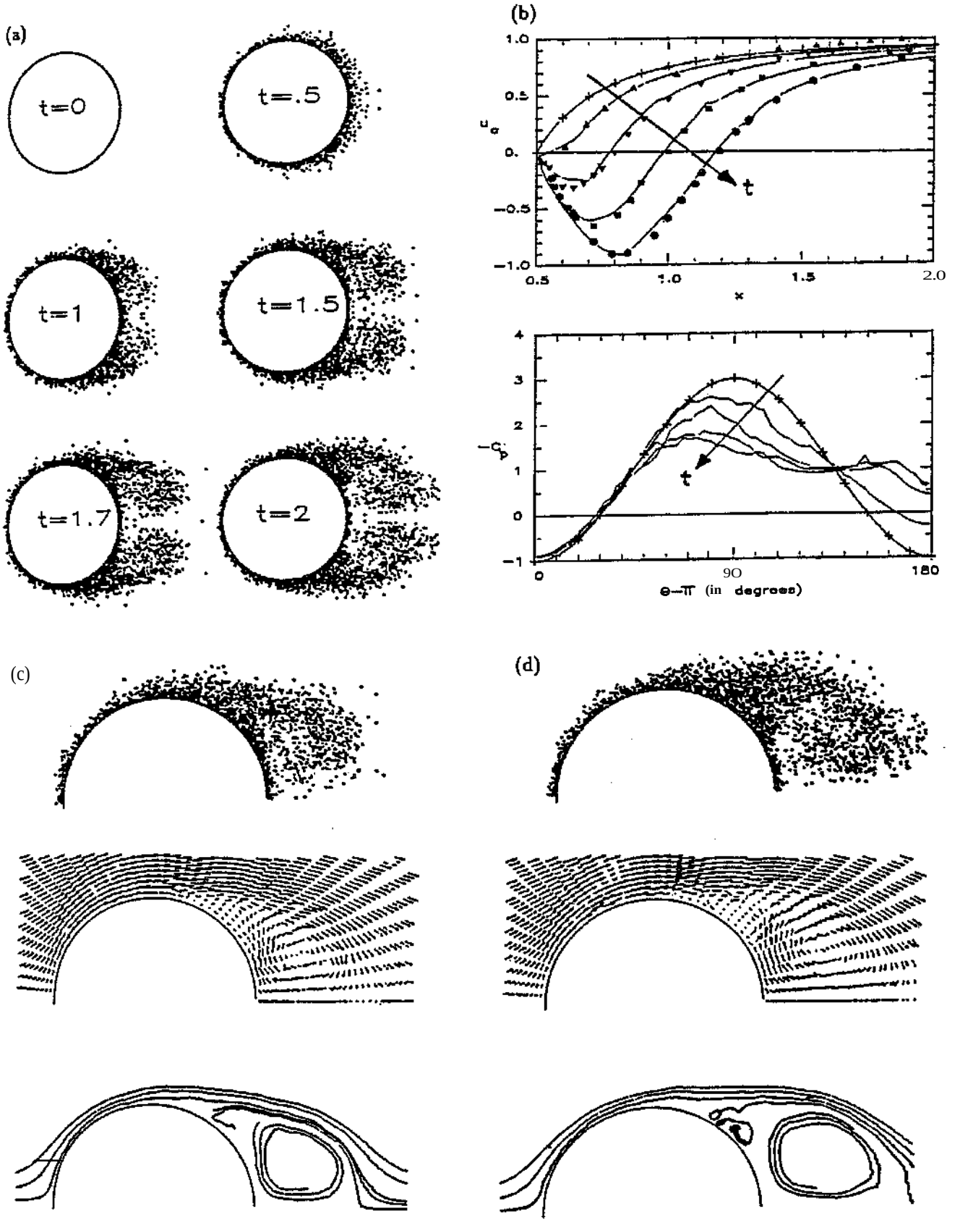

Fig. 5 Computed results for Re = 550. (a) Vortex patterns at times t, (b) distributions of streamwise centreline velocity u_c and pressure coefficient C_P at times t = 0.5, 1.0, 1.5, and 2.0 and comparison of vortex pattern, velocity vectors and particle traces at times (c) t = 1.5 and (d) t = 2.0. Symbols indicate experimental data (Bouard and Coutanceau 1980) for u_c and potential flow distribution for C_P.

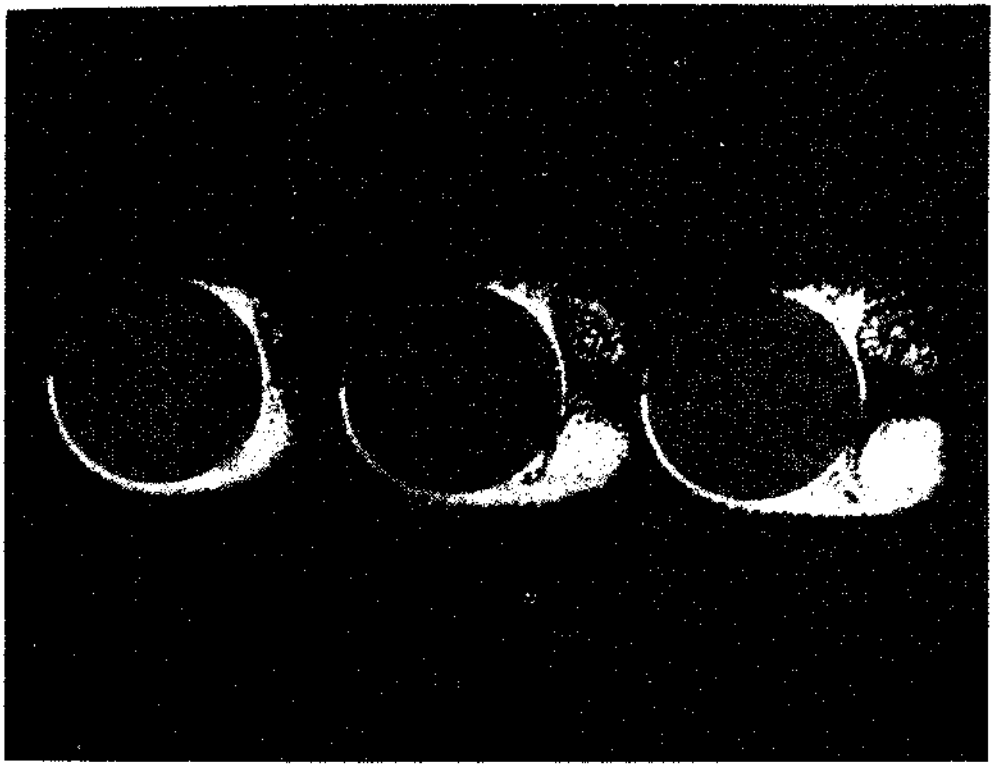

Figure 6. Evolution of vortex patterns around a two-dimensional circular cylinder at Re=3000. Patterns are shown at three time instants - (a) t = 1.0, (b) t = 1.5, and (c) t = 1.9.